



Discovery of endoplasmic reticulum calcium stabilizers to rescue ER-stressed podocytes in nephrotic syndrome

Sun-Ji Park^a, Yeawon Kim^a, Shyh-Ming Yang^b, Mark J. Henderson^b, Wei Yang^c, Maria Lindahl^d, Fumihiko Urano^e, and Ying Maggie Chen^{a,1}

^aDivision of Nephrology, Department of Medicine, Washington University School of Medicine, St. Louis, MO 63110; ^bNational Center for Advancing Translational Sciences, National Institutes of Health, Rockville, MD 20850; ^cDepartment of Genetics, Washington University School of Medicine, St. Louis, MO 63110; ^dInstitute of Biotechnology, University of Helsinki, Helsinki, Finland 00014; and ^eDivision of Endocrinology, Metabolism, and Lipid Research, Department of Medicine, Washington University School of Medicine, St. Louis, MO 63110

Edited by Martin R. Pollak, Beth Israel Deaconess Medical Center, Brookline, MA, and approved May 28, 2019 (received for review August 16, 2018)

Emerging evidence has established primary nephrotic syndrome (NS), including focal segmental glomerulosclerosis (FSGS), as a primary podocytopathy. Despite the underlying importance of podocyte endoplasmic reticulum (ER) stress in the pathogenesis of NS, no treatment currently targets the podocyte ER. In our monogenic podocyte ER stress-induced NS/FSGS mouse model, the podocyte type 2 ryanodine receptor (RyR2)/calcium release channel on the ER was phosphorylated, resulting in ER calcium leak and cytosolic calcium elevation. The altered intracellular calcium homeostasis led to activation of calcium-dependent cytosolic protease calpain 2 and cleavage of its important downstream substrates, including the apoptotic molecule procaspase 12 and podocyte cytoskeletal protein talin 1. Importantly, a chemical compound, K201, can block RyR2-Ser2808 phosphorylation-mediated ER calcium depletion and podocyte injury in ER-stressed podocytes, as well as inhibit albuminuria in our NS model. In addition, we discovered that mesencephalic astrocyte-derived neurotrophic factor (MANF) can revert defective RyR2-induced ER calcium leak, a bioactivity for this ER stress-responsive protein. Thus, podocyte RyR2 remodeling contributes to ER stress-induced podocyte injury. K201 and MANF could be promising therapies for the treatment of podocyte ER stress-induced NS/FSGS.

activating transcription factor 6 (ATF6), which act as proximal sensors of ER stress. ER stress activates these sensors by inducing phosphorylation and homodimerization of IRE1 α and PERK/eukaryotic initiation factor 2 α (eIF2 α), as well as relocalization of ATF6 to the Golgi, where it is cleaved by S1P/S2P proteases from 90 kDa to the active 50-kDa ATF6 (8), leading to activation of their respective downstream transcription factors, spliced XBP1 (XBP1s), ATF4, and p50ATF6 (8–10). The intense or prolonged UPR can result in cell apoptosis and death. Caspase 12, C/EBP homologous protein (CHOP), and Jun N-terminal kinase (JNK) are ER stress apoptotic pathways.

Mounting evidence has demonstrated that podocyte ER stress plays a vital role in the pathogenesis of idiopathic NS. In cell culture studies, certain NS-causing nephrin or podocin missense mutants are trapped inside the ER and activate ER stress (11–13). In mouse models, podocyte ER stress induced by the pathogenic mutation *Lamb2* C321R (14), *Actn4* K256E (15), or *Col4a3* G1332E (16) leads to NS and podocytopathy. In human studies, multiple collagen IV mutations, the most frequent mutations underpinning adult primary FSGS/steroid-resistant NS (17), activate the UPR in

endoplasmic reticulum stress | podocytes | type 2 ryanodine receptor | ER calcium stabilizer | K201

Primary nephrotic syndrome (NS), including focal segmental glomerulosclerosis (FSGS), is one of the leading causes of chronic kidney disease, which affects ~500 million people worldwide and is increasing in incidence (1). Seminal advances in past decades have identified primary NS/FSGS as a primary podocytopathy with major discoveries of podocyte-specific gene mutations in human NS patients, including *NPHS1*, *NPHS2*, *WT-1*, *LAMB2*, *CD2AP*, *TRPC6*, *ACTN4*, and *INF2*. Although accumulating studies have highlighted the importance of intracellular calcium dysregulation in the pathogenesis of podocytopathy, most studies have focused on increased calcium influx across the podocyte plasma membrane, resulting from overexpression of the G protein-coupled angiotensin II type 1 receptor (2) or hyperactivity/overexpression of transient receptor potential cation channel subfamily C member 6 (TRPC6) (3–5). The role of podocyte endoplasmic reticulum (ER) calcium efflux under ER stress in the pathogenesis of proteinuria remains to be elucidated.

The ER plays important roles in folding, posttranslational modification, and trafficking of newly synthesized secretory and membrane proteins. Protein folding is aided by ER-resident molecular chaperones and enzymes, such as Ig binding protein (BiP), calnexin, calreticulin, and protein disulfide isomerase (6, 7). Disturbance to ER homeostasis leads to accumulation of unfolded or misfolded proteins in the ER lumen, which causes ER stress and activates unfolded protein response (UPR) pathways. The UPR is regulated by 3 ER transmembrane proteins: inositol-requiring enzyme 1 (IRE1), protein kinase-like ER kinase (PERK), and

Significance

Podocyte injury is the hallmark of nephrotic syndrome (NS), a leading cause of chronic kidney disease affecting approximately 500 million people. We demonstrate that the podocyte endoplasmic reticulum (ER) calcium release channel, type 2 ryanodine receptor (RyR2), undergoes phosphorylation during ER stress. The accelerated podocyte ER calcium efflux due to leaky RyR2 activates cytosolic protease calpain 2, leading to podocyte injury. Most importantly, we have identified a chemical compound, K201, and a biotherapeutic protein, MANF, that can fix leaky RyR2 and inhibit podocyte injury. In addition, K201 can attenuate proteinuria in a podocyte ER stress-induced NS mouse model. The new class of drugs, podocyte ER calcium channel stabilizers, is an emerging therapeutic strategy to treat NS caused by ER dysfunction.

Author contributions: S.-J.P. and Y.M.C. designed research; S.-J.P. and Y.K. performed research; S.-M.Y., M.J.H., M.L., and F.U. contributed new reagents/analytic tools; S.-J.P., Y.K., W.Y., and Y.M.C. analyzed data; and S.-J.P. and Y.M.C. wrote the paper.

Conflict of interest statement: A provisional patent application entitled “Compositions and methods for treating and preventing endoplasmic reticulum (ER) stress-mediated kidney diseases” has been filed by Y.M.C., S.-J.P., Y.K., F.U. and the Washington University Office of Technology Management (serial no. 62/686705, filed on June 19, 2018). A provisional patent application entitled “Compositions and methods for treating and preventing endoplasmic reticulum (ER) stress-mediated kidney diseases” has been filed by Y.M.C., S.-J.P., Y.K., F.U. and the Washington University Office of Technology Management (serial no. 62/828514, filed on April 3, 2019).

This article is a PNAS Direct Submission.

Published under the PNAS license.

¹To whom correspondence may be addressed. Email: ychen@dom.wustl.edu.

This article contains supporting information online at www.pnas.org/lookup/suppl/doi:10.1073/pnas.1813580116/-DCSupplemental.

Published online June 24, 2019.

Podocyte lysates

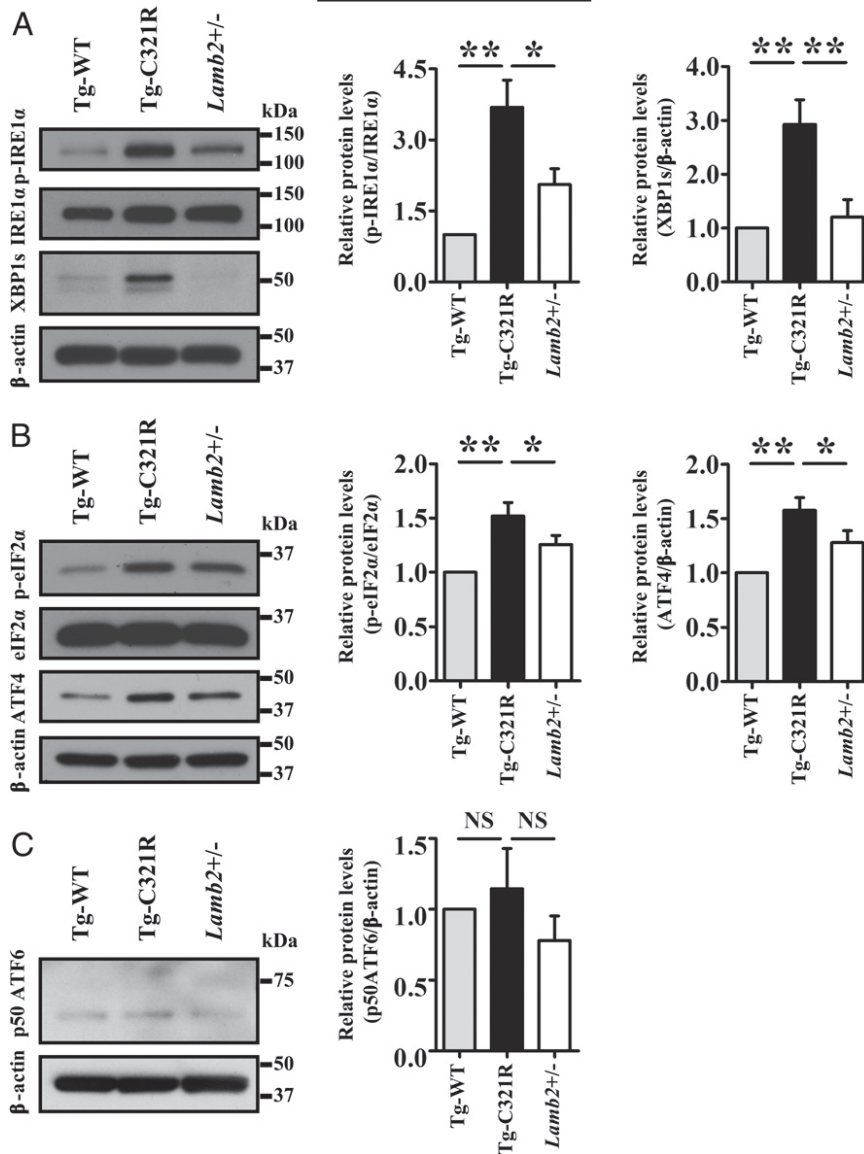


Fig. 1. ER stress induced by C321R-LAMB2 disparately regulates the UPR branches in podocytes at the early stage of NS. Primary podocytes (P1 or P2) were isolated and cultured from Tg-WT, Tg-C321R, and *Lamb2*^{+/-} mice at P27. (A) Representative immunoblots of p-IRE1α, IRE1α, and XBP1s expression in primary podocyte lysates of the indicated genotypes. A densitometry analysis of p-IRE1α normalized to IRE1α and XBP1s normalized to β-actin was performed in the podocyte lysates. (B) Representative immunoblots of p-eIF2α, eIF2α, and ATF4 expression in primary podocytes of the indicated genotypes. A densitometry analysis of p-eIF2α normalized to eIF2α and ATF4 normalized to β-actin was conducted in the podocyte lysates. (C) Representative immunoblot of p50ATF6 expression in primary podocytes of the indicated genotypes. A densitometry analysis of p50ATF6 normalized to β-actin was performed in the podocyte lysates. Quantification data represent the mean ± SD of 5 independent experiments. **P* < 0.05; ***P* < 0.01. NS, not significant by ANOVA.

podocytes (18). Moreover, in FSGS associated with *APOL1* renal risk alleles, ER stress secondary to altered endolysosomal trafficking has been shown to induce cell injury (19). Finally, CHOP is up-regulated in the podocytes of kidney biopsies from FSGS, membranous nephropathy (MN), and minimal change disease (MCD) patients compared with controls (20). Despite the importance of podocyte ER stress in NS, there is no treatment that targets the podocyte ER dysfunction.

Aberrant ER calcium homeostasis triggered by ER stress may play a critical role in the regulation of apoptotic cell death. Calcium in the ER lumen is maintained at concentrations 1,000- to 10,000-fold greater than in the cytoplasm by the sarco/ER Ca²⁺ adenosine triphosphatase (SERCA), a pump for uphill transport of Ca²⁺ from the cytoplasm into the ER lumen. The majority of calcium efflux from the ER is mediated by ryanodine receptors (RyRs) and inositol 1, 4, 5-triphosphate receptors (IP3Rs). Three isoforms of RyR and IP3R have been identified (21). In contrast to IP3Rs that are expressed in all cell types, RyRs are mainly expressed in muscles and neurons (21). RyR1 predominates in skeletal muscle, RyR2 predominates in heart and brain (22), and RyR3 is expressed at low levels in various tissues

(23). Whether these ER calcium channels undergo remodeling in ER-stressed podocytes and their functional impact in podocyte integrity and injury have not been studied.

To investigate the molecular pathogenesis and treatment of podocyte ER stress-induced NS, we have established a mouse model of NS caused by *LAMB2* C321R, a mutation identified in human patients (14). Laminin β2 encoded by *LAMB2* is a component of the laminin-521 (α5β2γ1) trimer, an important constituent of the mature glomerular basement membrane (GBM). Laminin trimerization occurs in the ER, and the trimers are secreted by both podocytes and glomerular endothelial cells to the GBM. We have shown that transgenic (Tg) expression of C321R-LAMB2 in podocytes via the podocyte-specific mouse nephrin promoter on the *Lamb2*^{-/-} background (*Lamb2*^{-/-};Tg-C321R, hereafter referred to as Tg-C321R mice) recapitulates features of the corresponding human NS patients (14). At 3–4 wk of age, when Tg-C321R mutants exhibit trace proteinuria without notable renal histological alterations, podocyte ER stress induced by the C321R mutant protein is evident (14, 24). At 6–8 wk of age, the mutant mice develop diffuse foot process (FP) effacement, mild GBM thickening, overt proteinuria, and FSGS

Podocyte lysates

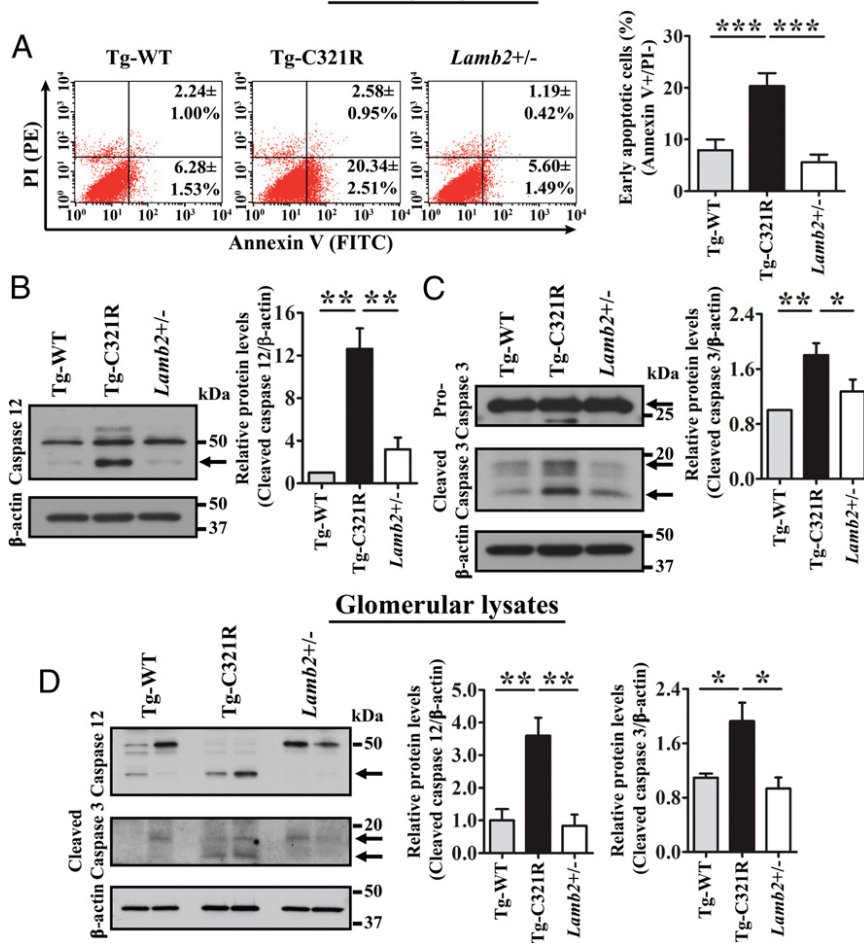


Fig. 2. Caspase 12 contributes to podocyte ER stress-mediated apoptosis at the early stage of NS. (A) Primary podocytes from Tg-WT, Tg-C321R, and *Lamb2*^{+/-} mice at P27 were stained with FITC-Annexin V and PI, and analyzed by flow cytometry. The values in the lower right quadrant of the representative histograms indicate the percentage of podocytes undergoing early apoptosis (Annexin V⁺/PI⁻ cells). The percentage of early apoptotic podocytes was expressed as the mean \pm SD from 3 independent experiments. ****P* < 0.001 by ANOVA. PE, phycoerythrin. (B and C) Primary podocyte lysates from Tg-WT, Tg-C321R, and *Lamb2*^{+/-} mice at P27 were analyzed by WB with the indicated antibodies. Arrows indicate cleaved forms of the proteins of interest. Quantification of cleaved caspase 12 (B), as well as cleaved caspase 3 (C), was normalized to β -actin. (D) Glomeruli were isolated from age-matched Tg-WT, Tg-C321R, and *Lamb2*^{+/-} mice at P27. Cleaved caspase 12, cleaved caspase 3, and β -actin were analyzed by WB in isolated glomeruli from the indicated genotypes. Quantification of cleaved caspase 12 and cleaved caspase 3 was normalized to β -actin in isolated glomerular lysates. Arrows indicate cleaved (active) caspases 12 and 3. Mean \pm SD of 5 independent experiments. **P* < 0.05, ***P* < 0.01 by ANOVA.

(14). We have also shown that in expression-matched *Lamb2*^{+/-};Tg-wild-type (WT) (hereafter referred to as Tg-WT) mice, expression of WT β 2 complementary DNA (cDNA) in podocytes is sufficient to restore the integrity of the glomerular filtration barrier and prevent proteinuria in *Lamb2*^{+/-} mice (25). By utilizing this monogenic NS mouse model, the aim of this study was to determine whether ER calcium homeostasis is dysregulated in podocytes undergoing ER stress and to discover novel therapeutic agents targeting at the ER to inhibit podocyte injury and proteinuria in NS/FSGS.

Results

Tripartite UPR Is Differentially Regulated in Mutant Podocytes in the Incipient Stage of NS. To delineate the molecular mechanism underpinning the regulation of the UPR in ER-stressed podocytes at the early stage of proteinuria, we isolated and cultured passage 0-1 (P0-P1) primary podocytes from Tg-WT, Tg-C321R, and *Lamb2*^{+/-} (WT) mice at postnatal day 27 (P27). Western blot (WB) analysis of primary podocytes showed that protein levels of phospho-IRE1 α (p-IRE1 α) and XBP1s, as well as phospho-eIF2 α (p-eIF2 α) and ATF4, were increased in Tg-C321R podocytes compared with the Tg-WT and WT podocytes (Fig. 1A and B). In contrast, the active form of ATF6 (p50 ATF6) was unchanged across genotypes, excluding its involvement in this disease model (Fig. 1C). Together, these data demonstrate that the IRE1 α and PERK pathways, but not the ATF6 pathway, are selectively activated in response to podocyte ER stress induced by the C321R mutation in the pathogenesis of NS.

Podocyte ER Stress Results in Caspase 12 Activation and Apoptosis at the Early Stage of the Disease. Chronic and unrelieved ER stress may result in apoptosis. Given that we had observed mild desmin expression in the mutant podocytes, an indicator of podocyte injury, at the early stage of proteinuria previously (14), we directly measured primary podocyte apoptosis at P27 by utilizing flow cytometry. Annexin V⁺/propidium iodide (PI)⁻ cells are regarded as early apoptotic cells, whereas double-positive cells are regarded as late apoptotic or necroptotic cells (26). Indeed, the rate of early apoptosis was significantly increased in Tg-C321R podocytes (20.34 \pm 2.51%) compared with Tg-WT (6.28 \pm 1.53%) and WT (5.60 \pm 1.49%) podocytes (*P* < 0.001) (Fig. 2A). We next investigated which ER stress-specific proapoptotic pathway was activated in the mutant podocytes at the early stage of disease. Besides CHOP activation in both Tg-C321R podocytes and glomeruli as shown by us before (24), a striking cleavage of ER-resident procaspase 12, reflecting its activation, was observed in Tg-C321R podocytes compared with control podocytes at P27 (Fig. 2B). Consequently, activation of the executioner caspase 3 (cleaved form of procaspase 3) was increased in the mutant podocytes versus control podocytes (Fig. 2C). To make sure that the observed activation of caspases 12 and 3 in mutant podocytes was not due to in vitro culturing, we also isolated glomeruli from the indicated genotypes at P27. The same results were confirmed in the isolated glomeruli from the different groups (Fig. 2D). On the other hand, the JNK pathway (p46/p54 kDa) was not involved in the podocyte ER stress-induced apoptosis at the early stage of proteinuria (SI Appendix, Fig. S1A and B). Taken together, these results demonstrate

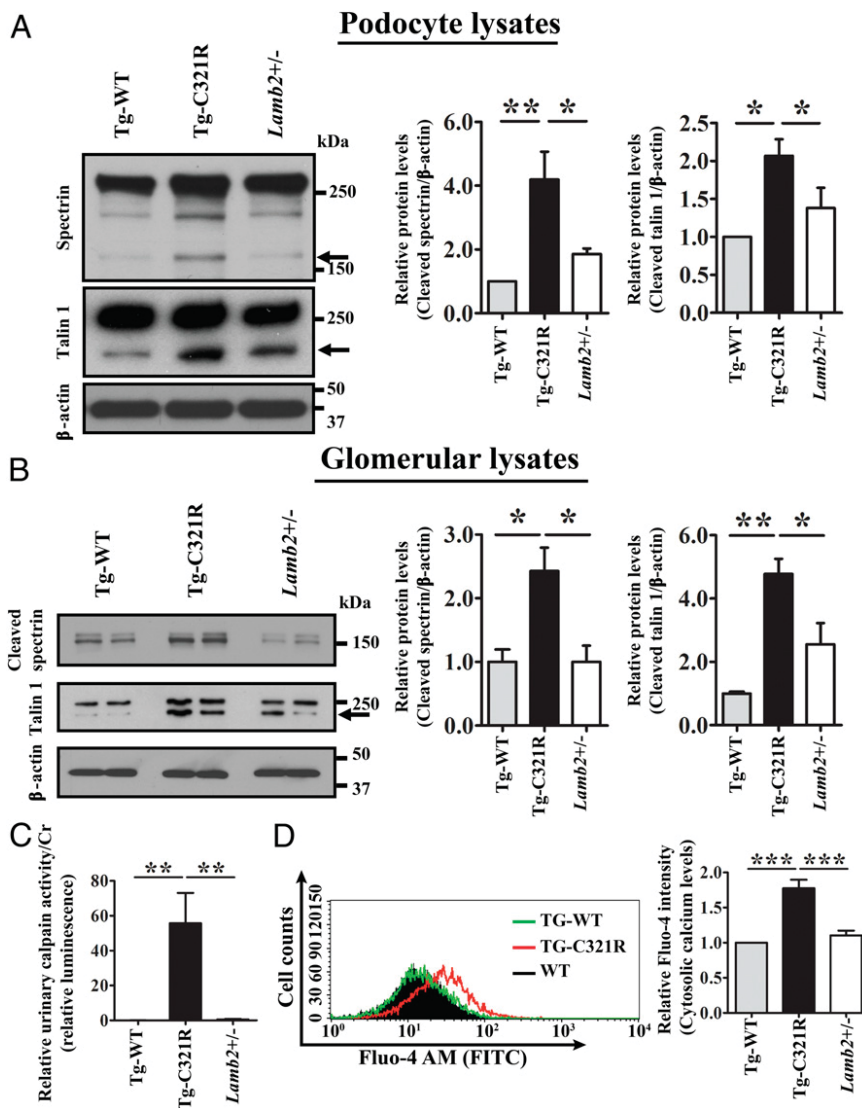


Fig. 3. Podocyte ER stress induces cytosolic calcium elevation and activation of calcium-dependent calpain 2 activity. (A) Primary podocyte lysates from Tg-WT, Tg-C321R, and *Lamb2*^{+/-} mice at P27 were analyzed by WB for cleavage of spectrin and talin 1. The arrows indicate cleaved spectrin or talin 1. Quantification of cleaved spectrin and talin 1 was normalized to β -actin in primary podocyte lysates. Mean \pm SD of 5 independent experiments. * P < 0.05, ** P < 0.01 by ANOVA. (B) Glomerular lysates from Tg-WT, Tg-C321R, and *Lamb2*^{+/-} mice at P27 were analyzed by WB for cleaved spectrin and talin 1. The arrow indicates cleaved talin 1. Quantification of cleaved spectrin and talin 1 was normalized to β -actin in glomerular lysates. Mean \pm SD of 5 independent experiments. * P < 0.05, ** P < 0.01 by ANOVA. (C) Urinary calpain activity/Cr was assayed from the indicated groups at P25–P27. The urinary calpain activity/Cr in *Lamb2*^{+/-} mice was set as 1 (n = 5 per group). ** P < 0.01 by ANOVA. (D) Tg-C321R and control podocytes were stained with the cytosolic calcium indicator Fluo-4 AM, and the fluorescence intensity was measured by flow cytometry. The relative fluorescence intensity was expressed as mean \pm SD from 3 independent experiments. *** P < 0.001 by ANOVA.

that caspase 12 contributes to podocyte ER stress-mediated apoptosis at the early stage of the disease pathogenesis.

Cytosolic Calcium-Dependent Calpain 2 Is Activated in Mutant Podocytes.

Activation of ER-resident procaspase 12 in the mutant podocytes (Fig. 2 *B* and *D*) prompted us to further determine its upstream calpain 2 activity at the early stage of proteinuria. Calpain 2 is a cytosolic cysteine protease, which is known to be activated by calcium elevation and cleaves caspase 12 after activation. Additionally, calpain 2 has been shown to mediate diverse biological functions, including cleavage of podocyte cytoskeleton-associated anchoring protein talin 1, leading to FP effacement (27). WB revealed that Tg-C321R podocytes exhibited increased cleavage of alpha II spectrin, a well-characterized substrate for calpain 2 and a component of the nephrin multiprotein complex (28), compared with control podocytes at P27, indicative of the enhanced activity of calpain 2 and cytosolic calcium overload in Tg-C321R podocytes (Fig. 3*A*). Meanwhile, increased cleavage of talin 1 was also noted in Tg-C321R podocytes compared with control podocytes at P27 (Fig. 3*A*). We further verified increased cleavage of spectrin and talin 1 in Tg-C321R glomeruli compared with control glomeruli at P27 (Fig. 3*B*). As calpain 2 is secreted from podocytes to the urine (29), urinary calpain activity was determined by luciferase assay, and normalized to urine creatinine (Cr) excretion (urinary calpain

activity/Cr) in Tg-WT, Tg-C321R, and *Lamb2*^{+/-} mice at P25–P27. As shown in Fig. 3*C*, the urinary calpain activity/Cr in Tg-C321R mutants was significantly higher than that in control mice. We next thought to demonstrate that cytosolic calcium was increased in the mutant podocytes directly. Podocytes were stained with the fluorescent cytosolic calcium indicator Fluo-4 AM (acetoxymethyl), and the fluorescence intensity was measured by flow cytometry. As shown in Fig. 3*D*, cytoplasmic calcium levels were higher in Tg-C321R podocytes relative to control podocytes. Collectively, these results indicate that the calpain 2-caspase 12 pathway was activated by cytosolic calcium elevation in the mutant podocytes, resulting in the subsequent podocyte injury.

Phosphorylation of RyR2 Contributes to Podocyte ER Calcium Depletion in Mutant Podocytes.

To gain insight into the mechanism underlying intracellular calcium dysregulation in the mutant podocytes undergoing ER stress, we performed RNA sequencing of primary podocytes (passage 0) isolated from Tg-WT and Tg-C321R mice at P27. Gene set enrichment analysis (GSEA) (30) revealed that expression of genes involved in calcium signaling was significantly increased in Tg-C321R podocytes compared with Tg-WT podocytes (Fig. 4*A*). The detailed profile, including gene rank in gene list, rank metric score, running enrichment score, and core enrichment, is included in *SI Appendix, Table S1*. Furthermore,

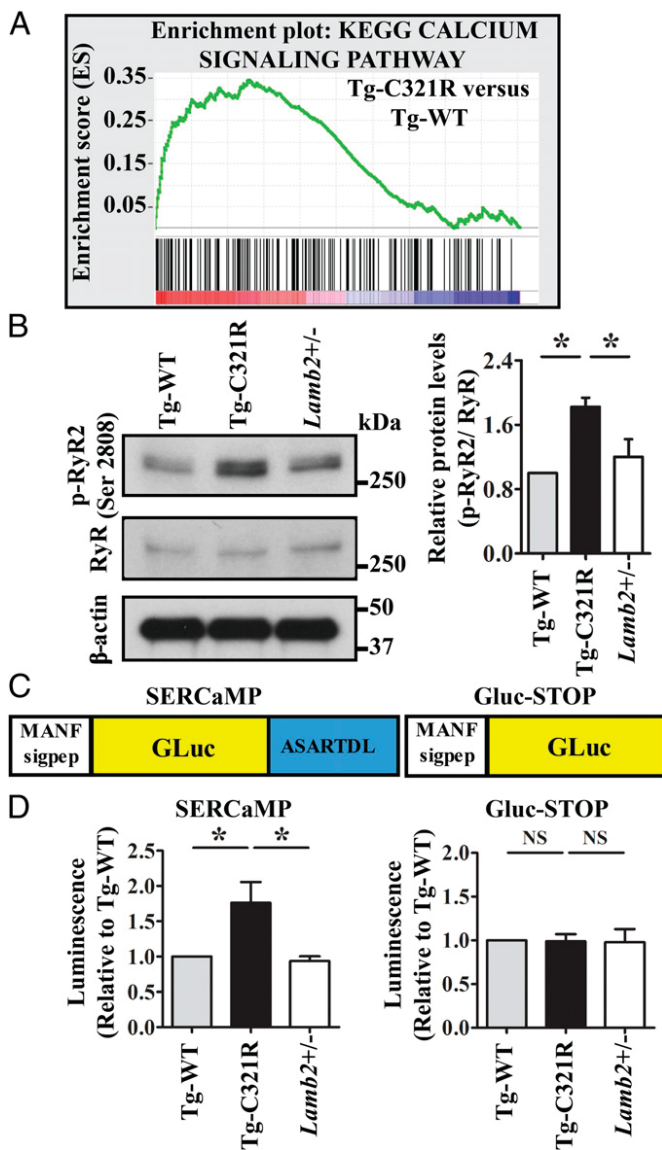


Fig. 4. Podocyte ER stress induces ER calcium release through RyR2 phosphorylation. (A) GSEA of calcium-signaling gene transcript abundance in primary podocytes (P0) isolated from Tg-C321R and Tg-WT mice at P27 (enrichment score = 0.34, normalized enrichment score = 1.41). $P < 0.001$. (B) WB analysis of phospho-RyR2 (p-RyR2; Ser2808) and RyR expression in primary podocyte lysates from the indicated genotypes. Quantification of p-RyR2 (Ser2808) was normalized to RyR in the podocyte lysates. Mean \pm SD of 3 independent experiments. $*P < 0.05$ by ANOVA. (C) Schematic of SERCaMP and control GLuc-STOP fusion proteins. The first 18 amino acids of GLuc (MGVKVLFALICIAVAEAK, signal peptide) were replaced with the signal peptide of MANF (amino acids 1–23, MWATQGLAVALALSVLPGSRALR) to target the proteins to the secretory pathway. The C-terminal sequence of MANF, ASARTDL, was fused to GLuc. (D) Primary podocytes from Tg-WT, Tg-C321R, and *Lamb2*^{+/-} mice at P27 were transduced with lentivirus expressing SERCaMP or GLuc-STOP. Forty-eight h after the virus infection, luciferase activity was measured in the medium and normalized to the value in Tg-WT mice. Mean \pm SD from 3 independent experiments. $*P < 0.05$. NS, not significant by ANOVA.

Kyoto Encyclopedia of Genes and Genomes (KEGG) calcium-signaling pathway analysis showed that RyR and SERCA expression was up-regulated and that IP3R was down-regulated in the mutant podocytes versus Tg-WT podocytes (SI Appendix, Fig. S2), suggesting that aberrant RyR may mediate ER calcium leak, contributing to cytosolic calcium overload in podocytes under ER

stress. We next looked at RyR expression at the protein level. WB did not reveal a difference in RyR expression among the different groups by using an anti-RyR antibody that recognizes all 3 isoforms of RyR (Fig. 4B). Because it has been shown that the RyR2 isoform is present in the rabbit kidney cortex (31) and its activity is modulated by phosphorylation of the channel (32), we further examined phosphorylation of RyR2 at Ser2808. In cardiomyocytes, chronic hyperphosphorylation of RyR2-Ser2808 in heart failure and ventricular arrhythmia has been shown to be critical in causing diastolic sarcoplasmic reticulum calcium leak by destabilizing the closed state of the channel (32–34). Indeed, mutant podocytes showed increased phosphorylation of RyR2 at Ser2808 compared with control podocytes at the early stage of disease (Fig. 4B). Finally, to demonstrate that ER calcium was depleted due to augmented ER calcium release in live podocytes, we monitored podocyte ER calcium homeostasis by utilizing the secreted ER calcium-monitoring protein (SERCaMP) assay (35). It has been shown that the carboxyl-terminal sequence of an ER stress protein mesencephalic astrocyte-derived neurotrophic factor (MANF), ASARTDL, is sufficient to specifically confer ER calcium depletion-dependent secretion (36). In SERCaMP, ASARTDL is appended to an unrelated secreted protein, *Gaussia* Luciferase (GLuc), and the first 18 amino acids of GLuc were replaced with the signal peptide of MANF to target GLuc to the secretory pathway (35, 37) (Fig. 4C). The GLuc-based SERCaMP is localized to the lumen of the ER under normal conditions, whereas it is secreted specifically in response to ER calcium depletion (35). When human embryonic kidney (HEK) 293T cells stably expressing SERCaMP or control GLuc-STOP without the ASARTDL tag were treated with dimethyl sulfoxide (DMSO) or 0.1 μ M thapsigargin (TG), a SERCA inhibitor causing ER calcium depletion for 6 h, SERCaMP secretion, as measured by luciferase activity in the cell culture medium, was increased in response to ER calcium depletion induced by TG (SI Appendix, Fig. S3). Importantly, when equal numbers of Tg-C321R as well as control Tg-WT and WT primary podocytes, which were isolated from the respective mice at P27, were transduced with lentivirus expressing SERCaMP or GLuc-STOP for 48 h, luciferase assay showed that secreted SERCaMP by Tg-C321R podocytes was significantly increased compared with that by control podocytes (Fig. 4D). In contrast, secretion of untagged GLuc did not differ among the different genotypes (Fig. 4D). In summary, these data demonstrate that podocyte RyR2 hyperphosphorylation is one molecular mechanism mediating the accelerated podocyte ER-to-cytosol calcium efflux and ER calcium depletion before significant proteinuria.

Identification of K201 as a Podocyte ER Calcium Stabilizer. We next tested the effect of a previously reported ER calcium release inhibitor K201, which is known to stabilize the closed state of RyR2 in cardiomyocytes during heart failure or cardiac arrhythmia (33), on podocytes. First, we confirmed that K201 can abrogate TG-induced ER calcium depletion in HEK 293T cells (SI Appendix, Fig. S4). Then, primary podocytes isolated and cultured from Tg-WT and Tg-C321R mice at P27 were treated with K201 at 5 μ M for 24 h. As shown in Fig. 5A, K201 markedly blocked the increased podocyte ER-to-cytosol calcium leak in Tg-C321R podocytes, as measured by the cytosolic calcium indicator Fluo-4. Mechanistically, treatment with K201 inhibited hyperphosphorylation of RyR2 at Ser2808 in the mutant podocytes (Fig. 5B). Consequently, K201 suppressed overactivation of calpain 2, as indicated by the decreased cleavage of alpha II spectrin, as well as cytoskeletal protein talin 1, in the mutant podocytes (Fig. 5C). Furthermore, K201 treatment abolished its downstream activation of procaspases 12 and 3 in the ER-stressed podocytes (Fig. 5D). Ultimately, K201 significantly decreased the early apoptotic rate in Tg-C321R podocytes (Annexin V⁺/PI⁺ cells) from $24.73 \pm 2.22\%$ to $15.23 \pm 2.84\%$ ($P < 0.05$) (Fig. 5E). The higher apoptotic rates in all groups were most likely due to the effect of

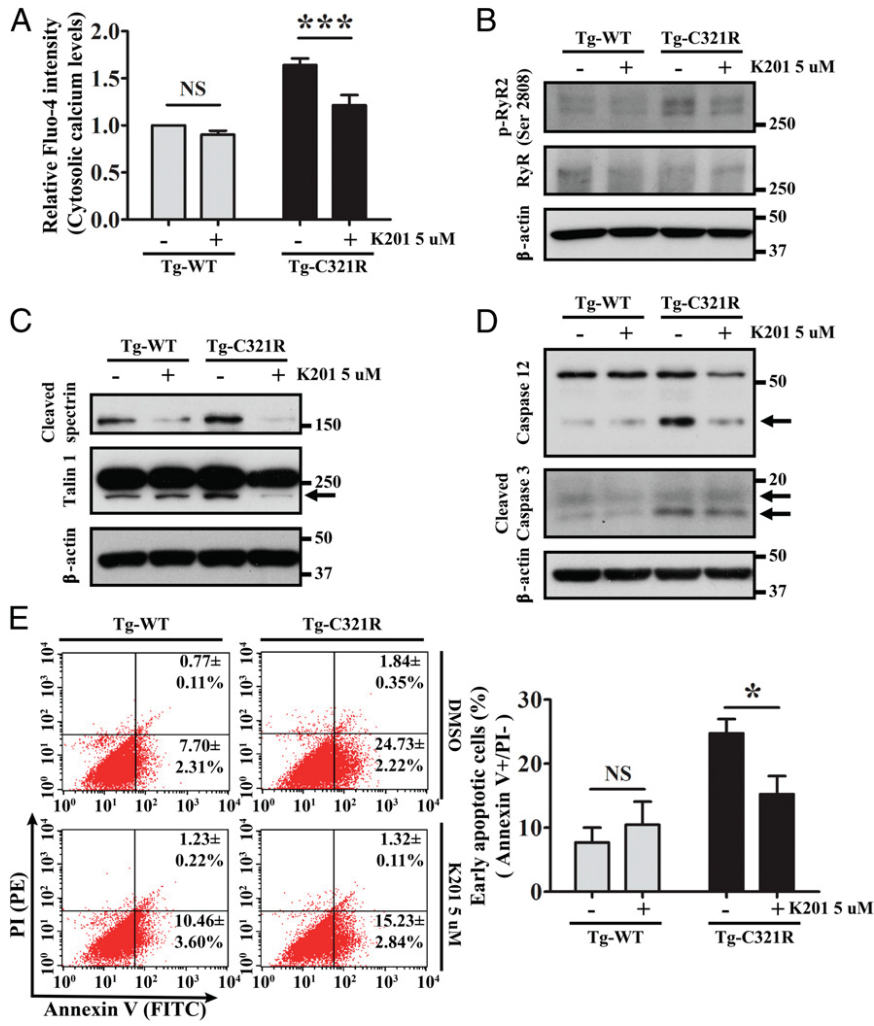


Fig. 5. K201 attenuates ER calcium release, downstream calpain 2-caspase 12 activation, and apoptosis in Tg-C321R podocytes. Cultured primary podocytes from Tg-WT and Tg-C321R mice at P27 were treated with 5 μ M K201 or DMSO (vehicle control) for 24 h. (A) Cytosolic calcium levels in DMSO- and K201-treated podocytes were measured by the cytosolic calcium indicator Fluo-4. Mean \pm SD of 3 independent experiments. *** P < 0.001 by ANOVA. Podocyte lysates treated with or without K201 were analyzed by WB for levels of phospho-RyR2 (p-RyR2; Ser2808) and RyR (B), cleaved spectrin and talin 1 (C), and cleaved caspase 12 and caspase 3 (D). Arrows indicate cleaved proteins. (E) Podocyte early apoptotic rate in the presence or absence of K201 was assessed by flow cytometry analysis of Annexin V⁺/PI⁻ podocytes. The percentage of early apoptotic cells was expressed as mean \pm SD from 3 independent experiments. PE, phycoerythrin. * P < 0.05 by ANOVA. NS, not significant by ANOVA.

DMSO. These results provide direct measurements of the effects of K201 in ameliorating podocyte ER stress-induced calcium leak and protecting against apoptosis in primary podocytes under ER stress.

To further demonstrate that leaky podocyte RyR2 is an important drug target to induce podocyte injury and that restoring disrupted podocyte ER calcium homeostasis by the RyR2 modulator K201 is therapeutically beneficial, we determined the efficacy of K201 in vivo. At 3 wk of age, when Tg-C321R mutants had developed very mild albuminuria, a cohort of Tg-C321R mice ($n = 12$) and control *Lamb2*^{+/-} littermates ($n = 16$) was injected intraperitoneally with K201 or vehicle. Vehicle was 20% (2-hydroxypropyl)- β -cyclodextrin (HBC), a commonly used nontoxic solubilizer for lipophilic drugs. K201 (12.5 mg/kg in the first week when the weight of mice was around 10 g or 15 mg/kg afterward) and 20% HBC were administered once daily 5 d in a row in a week over a course of 4 wk. Urinary calpain activity/Cr was dramatically decreased in K201-treated Tg-C321R mutants compared with 20% HBC-treated mutant mice as early as 2 wk after the treatment, and continued to be suppressed by K201 at 4 wk post-treatment (Fig. 6A), indicating that K201 injection effectively blocks ER calcium leak in Tg-C321R podocytes in vivo. Subsequently, K201 treatment significantly reduced albuminuria at 3 wk (0.095 ± 0.029 versus 0.137 ± 0.037 g/mg of Cr) and 4 wk (0.098 ± 0.016 versus 0.142 ± 0.022 g/mg of Cr) postinjection (Fig. 6B), as well as improved kidney function as indicated by blood urea nitrogen (BUN) at the end of 4 wk of injection (Fig. 6C). Meanwhile, no abnormality of renal function (Fig. 6C) or kidney histology (SI

Appendix, Fig. S5) was noted in K201-treated mice compared with vehicle-treated control littermates. Together, our study shows that the podocyte ER RyR2 stabilizer K201 can antagonize podocyte ER stress-induced enhanced ER calcium release and proteinuria.

Discovery of MANF as an ER Calcium Channel Stabilizer. MANF, a newly identified 18-kDa soluble protein, is up-regulated in response to experimental ER stress in various cell types (38–40). It is retained in the ER by calcium-dependent interaction with BiP, and selectively secreted upon ER calcium depletion (36, 37). Whether secreted MANF can, in turn, maintain the ER calcium homeostasis has not been investigated. Previously, we have shown that ER stress induced MANF expression at both transcriptional and translational levels in Tg-C321R podocytes in the early stage of proteinuria (24). We next assessed the impact of MANF on primary podocytes isolated from Tg-WT and Tg-C321 mice at P27. When control and Tg-C321R podocytes were treated with MANF recombinant protein (5 μ g/mL) for 24 h, cytosolic calcium levels in the mutant podocytes were significantly decreased after the treatment (Fig. 7A), which is consistent with reduced phosphorylation of ER RyR2 following MANF treatment (Fig. 7B). As a result, Tg-C321R podocytes treated with MANF showed inhibition of calpain 2 activation, as demonstrated by decreased cleavage of spectrin and talin 1 (Fig. 7C), as well as suppression of active cleaved caspase 12 compared with untreated Tg-C321R podocytes (Fig. 7D). In addition, CHOP induction in MANF-treated Tg-C321R podocytes was abrogated compared with untreated mutant podocytes (Fig.

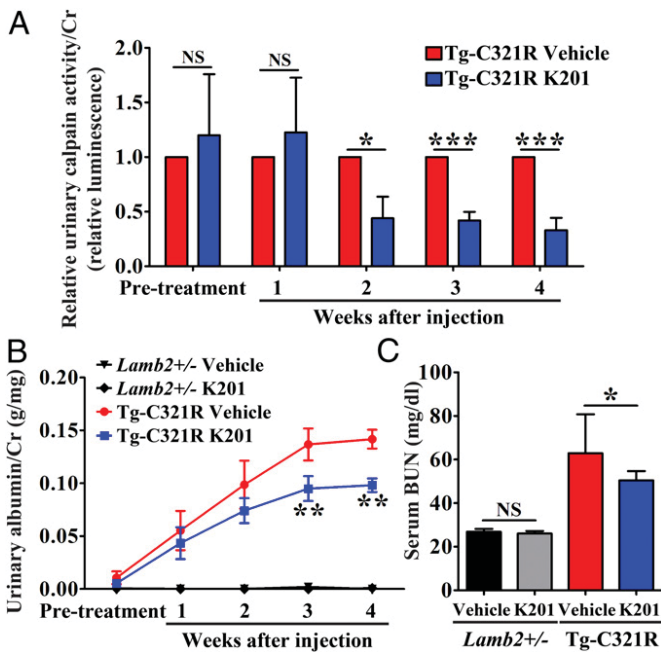


Fig. 6. K201 mitigates podocyte ER stress-mediated proteinuric kidney disease progression. (A) K201 inhibits urinary calpain activity in Tg-C321R mice after 2 wk of injection. Urinary calpain activity/Cr was measured by luciferase assay from both K201- and 20% HBC-treated Tg-C321R mice at pretreatment (P17–P19) and at weekly intervals posttreatment. The urinary calpain activity/Cr in the 20% HBC-treated Tg-C321R mice at the respective time points was set as 1 ($n = 6$ per group). * $P < 0.05$, *** $P < 0.001$ by t test. (B) K201 (12.5–15 mg/kg, once daily, 5 d per week) by intraperitoneal injection attenuates albuminuria in Tg-C321R mutants treated for 4 wk when administered at 3 wk of age. The pretreatment albuminuria was measured at P17–P19 ($n = 6$ per group for vehicle or K201-injected Tg-C321R mice and $n = 8$ per group for vehicle or K201-injected *Lamb2^{+/-}* mice). Mean \pm SD. ** $P < 0.01$ by ANOVA. (C) Serum BUN of the indicated groups following 4 wk of K201 or 20% HBC treatment ($n = 6$ per group for vehicle or K201-injected Tg-C321R mice and $n = 8$ per group for vehicle or K201-injected *Lamb2^{+/-}* mice). Mean \pm SD. * $P < 0.05$. NS, not significant by ANOVA.

7D). Since the CHOP gene promoter contains binding sites for the master transcription factors XBP1s and ATF4 that were induced in the ER-stressed podocytes (Fig. 1 A and B), we therefore reasoned that MANF might suppress the induction of these 2 transcription factors in the mutant podocytes. Indeed, we observed an inhibition of both XBP1s and ATF4 by MANF in the mutant podocytes (Fig. 7E). In agreement with the suppression of both caspase 12 and CHOP proapoptotic pathways in Tg-C321R podocytes, MANF treatment substantially attenuated early apoptotic rate (Annexin V⁺/PI⁻) in the mutant podocytes from $17.18 \pm 0.77\%$ to $10.09 \pm 0.51\%$ ($P < 0.05$) at the early stage of disease (Fig. 7F). These data show that besides stabilizing ER calcium release channel RyR2, MANF has pleiotropic prosurvival effects to rescue ER-stressed podocytes.

Discussion

The present study shows that hyperphosphorylation of RyR2 in ER-stressed podocytes contributes to increased podocyte ER calcium efflux, leading to downstream activation of the calpain 2-caspase 12 proapoptotic pathway at an early stage of NS. Our findings have identified an important therapeutic target, ER calcium release channel RyR2 in podocytes, which is involved in podocyte injury. Most importantly, we have successfully identified a RyR2 inhibitor K201, which can suppress podocyte ER calcium leak and subsequent calpain 2-caspase 12 overactivation in podocytes under ER stress, as well as ameliorate proteinuria

in our podocyte ER stress-induced monogenic NS mouse model. We have also discovered that MANF can normalize RyR2 phosphorylation status and antagonize podocyte apoptosis in addition to other prosurvival effects. Thus, we have identified a chemical compound and a biotherapeutic protein belonging to a class of drugs, podocyte ER calcium channel stabilizers, that can fix leaky RyR2 in ER-stressed podocytes and mitigate proteinuria (Fig. 8).

RyR2 is a homotetramer comprising 4 monomers, each containing a transmembrane segment (41). RyR2 has an enormous cytoplasmic domain that serves as a scaffold for regulator proteins that modulate the channel's activity (42). The RyR2 cytoplasmic scaffold domain contains kinases (protein kinase A and calcium/calmodulin-dependent kinase A), phosphatases (protein phosphatase 1 and 2a), and Ca²⁺ channel-stabilizing subunit calstabin-2, as well as other modulatory proteins, including phosphodiesterase 4D3, which degrades cyclic adenosine monophosphate (cAMP) and thus inhibits cAMP-dependent protein kinase A activation (43). Protein kinase A and calcium/calmodulin-dependent kinase A can both phosphorylate different sites (Ser2808, Ser2809, Ser2814, Ser2815, and Ser2030). Mimicking constitutive phosphorylation of RyR2 at Ser2808 in RyR2^{S2808D/S2808D} mice is associated with depletion of calstabin-2, elevated RyR2 oxidation, and nitrosylation, resulting in increased diastolic sarcoplasmic reticulum calcium leak in cardiomyocytes. The mice developed age-dependent cardiomyopathy and exhibited increased mortality after myocardial infarction compared with WT littermates. Whether the mutant mice have an altered kidney phenotype was not reported (33). In contrast, genetic ablation of RyR2 phosphorylation at Ser2808 in RyR2^{S2808A/S2808A} mice prevents remodeling of the RyR2 macromolecular complex (32). These mice are protected against chronic catecholaminergic-induced cardiac dysfunction (34) and development of heart failure after myocardial infarction (32), as well as against stress-induced cognitive dysfunction (44). Here, we have shown that defective RyR2 channel function due to hyperphosphorylation at Ser2808 in ER-stressed podocytes may be one molecular mechanism underlying the aberrant ER calcium release that can cause podocyte apoptosis and injury. Thus, inhibition of podocyte RyR2 leak is an attractive therapeutic strategy for the treatment of primary NS induced by podocyte ER stress.

K201, also known as JTV-519, is a derivative of 1, 4-benzothiazepine that has been shown to stabilize the closed state of RyR2 in cardiomyocytes, thus reducing heart failure progression and ventricular arrhythmia by inhibiting diastolic sarcoplasmic reticulum calcium leak (33, 45). The investigational drug that was studied in clinical trials for treatment of arrhythmia as well as protection against acute myocardial infarction has an outstanding in vivo safety profile (43). In the current study, we are repurposing K201 to treat ER stress-induced podocytopathy. In addition to inhibiting phosphorylation of RyR2-Ser2808, K201 may exert additional therapeutic effects in correcting the maladaptive remodeling of podocyte RyR2. Other components of the RyR2 macromolecular complex, including protein kinases, phosphatases, calstabin-2, and phosphodiesterase 4D3, warrant further examination.

In the present study, we have also discovered that MANF reduces phosphorylation of RyR2 at Ser2808 and confers protection from the detrimental effects of increased ER calcium efflux in podocytes. It has been found that MANF can mitigate diabetes (46), exert neurotrophic function in Parkinson's disease (47, 48), protect cardiac myocytes in myocardial infarction (36), reduce cortical neuron injury in ischemic stroke (49, 50), and promote macrophage phenotype switch from proinflammatory to prorepair antiinflammatory macrophages (51) in animal models. We have recently shown that MANF is a urinary biomarker for ER stress-mediated kidney diseases (24). However, the biological function of this protein has not been studied in kidney disease, and the cytoprotective mechanisms remain obscure. Consistent with previous reports that MANF modulates ER

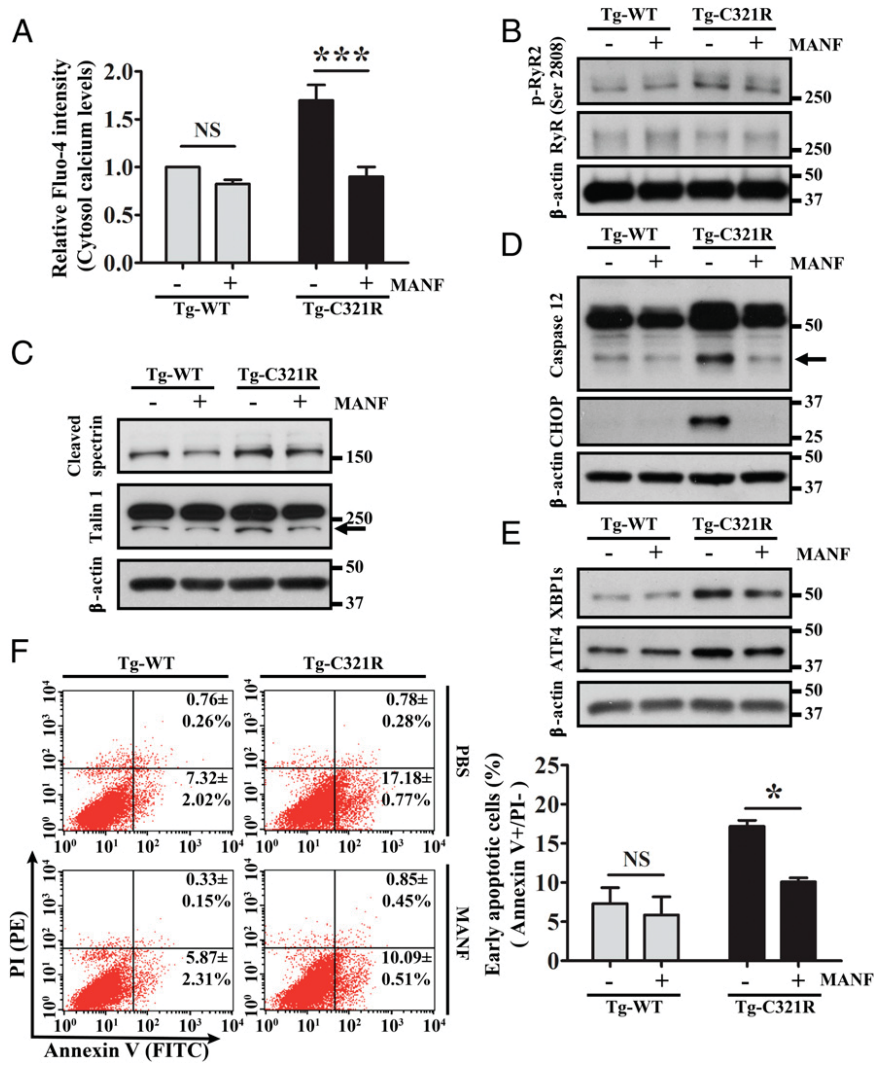


Fig. 7. Recombinant MANF inhibits both calcium-dependent and -independent apoptotic pathways in ER-stressed podocytes. Primary podocytes isolated from Tg-WT and Tg-C321R mice at P27 were treated with 5 μ g/mL recombinant MANF or PBS (control) for 24 h. (A) Cytosolic calcium levels in Tg-WT and Tg-C321R podocytes were measured by the cytosolic calcium indicator Fluo-4 in the presence or absence of recombinant MANF. Mean \pm SD of 3 independent experiments. *** P < 0.001 by ANOVA. Immunoblot analysis monitoring phosphor-RyR2 (p-RyR2; S2808) and RyR (B), cleaved spectrin and talin 1 (C), active caspase 12 and CHOP (D), and XBP1s and ATF4 in control and Tg-C321R podocytes treated with or without MANF (E) was performed. Arrows indicate cleaved proteins. (F) Podocytes undergoing early apoptosis (Annexin V⁺/PI⁻ cells) in the presence or absence of MANF were detected by flow cytometry. The percentage of early apoptotic cells was expressed as mean \pm SD from 3 independent experiments. PE, phycoerythrin. * P < 0.05 by ANOVA. NS, not significant by ANOVA.

stress-signaling branches and inhibits CHOP induction in animal models of cerebral ischemia and diabetes, respectively (46, 52), we also found that MANF attenuates the up-regulation of ER-signaling arms IRE1 α -XBP1s and PERK-eIF2 α -ATF4, as well as suppressing the ER calcium depletion-independent CHOP apoptotic pathway. In addition, MANF acts on dysfunctional podocyte RyR2 channels to inhibit Ser2808 phosphorylation and

calcium leak. Further studies will be performed to determine the molecular mechanism underpinning the protective effect of MANF on the malfunctioning ER calcium release channel in podocytes. We will also generate podocyte-specific MANF Tg mice to examine in vivo effects of MANF on podocyte ER dysfunction and proteinuria.

In conclusion, our study provides a mechanism for treating podocyte ER stress-induced proteinuria that targets podocyte leaky RyR2 channels. Based on our proof-of concept studies, we envision that development of podocyte RyR2 stabilizers may have wide clinical applications in the treatment of podocyte ER stress-induced hereditary or sporadic podocytopathies, including hereditary NS, FSGS, MN, MCD, Alport syndrome, or diabetic nephropathy, which may share a common feature of having “druggable” dysregulated RyR2 in podocytes.

Materials and Methods

Mice. Tg-WT, Tg-C321R, and *Lamb2*^{-/-} mice have all been described previously (14, 24). All animal experiments conformed to the *NIH Guide for the Care and Use of Laboratory Animals* (53) and were approved by the Washington University Animal Studies Committee.

Isolation of Mouse Glomeruli. Mice were perfused through the heart with magnetic 4.5- μ m-diameter Dynabeads (Invitrogen). Kidneys were minced into small pieces, digested by collagenase A (Sigma-Aldrich) and DNase I (Sigma-Aldrich), filtered, and collected using a magnet. The purity of glomeruli was >95%.

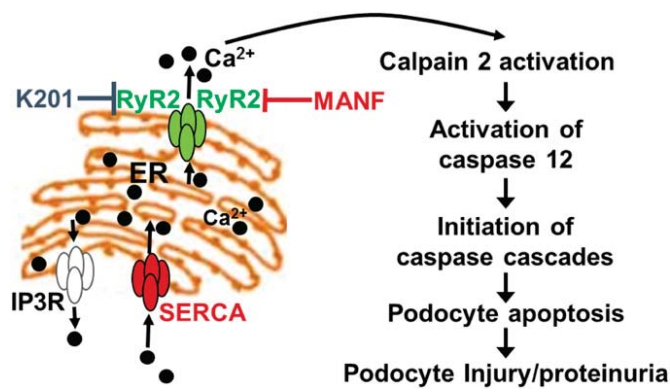


Fig. 8. Modulation of podocyte ER calcium depletion-induced apoptosis and injury by K201 and MANF.

Mouse Primary Podocyte Culture. Isolated glomeruli from Tg-WT, Tg-C321R, and *Lamb2*^{+/-} mice at P27 were plated onto collagen type I-coated culture dishes, and cultured in 5% CO₂ at 37 °C in Dulbecco's modified Eagle's medium (DMEM)/Ham's F-12 (2:1) that contained 3T3-L1 supernatant, 5% heat-inactivated fetal bovine serum (FBS; Gibco), 1% Insulin-Transferrin-Selenium liquid media supplement (Gibco), and 100 U/mL penicillin-streptomycin (Gibco). After 3 d, cell colonies began to sprout around the glomeruli. These cells [passage 0 (P0)] showed an epithelial morphology with a polyhedral shape when confluence was reached. P0 podocytes from the indicated genotypes were used for RNA sequencing, and P1 and P2 podocytes were used for other in vitro studies.

Antibodies and Reagents. Commercially available antibodies were obtained as follows: anti-caspase 12, anti-caspase 3, anti-p-JNK, anti-JNK, anti-p-eIF2 α , anti-eIF2 α , and anti-IRE1 α antibodies were from Cell Signaling; anti-ATF6 and anti-p-IRE1 α antibodies were from Novus Biological; anti-CHOP antibody was from Thermo Fisher Scientific; anti-XBP1s antibody was from BioLegend; anti-talin 1 and anti-spectrin α -chain antibodies were from Millipore; anti-ATF4 antibody was from Santa Cruz Biotechnology, anti-RyR and anti-phospho-RyR2 (S2808) antibodies were from Abcam; and horseradish peroxidase (HRP)-conjugated anti- β -actin antibody was from Sigma-Aldrich. HRP-conjugated anti-mouse and anti-rabbit secondary antibodies were from Santa Cruz Biotechnology. Rat collagen 1 was from Trevigen. Fluo-4 AM was purchased from Invitrogen, and probenecid was from Santa Cruz Biotechnology. Recombinant human MANF was from R&D Systems. K201 was produced by the NIH/National Center for Advancing Translational Sciences (NCATS).

WB Analysis. Mouse primary podocytes and isolated glomeruli were lysed by radioimmunoprecipitation assay buffer (Cell Signaling) containing protease inhibitor mixture (Sigma-Aldrich) and phosphatase inhibitor tablets (Roche). The protein concentrations of cell and glomerular lysates were determined by Bio-Rad Protein assay using bovine serum albumin as a standard. Denatured proteins were separated on sodium dodecyl sulfate (SDS)-polyacrylamide gels and then transferred to polyvinylidene difluoride membranes (Thermo Fisher Scientific). The membranes were blocked with 5% nonfat milk for 1 h and then incubated overnight with primary antibodies. Following incubation, membranes were washed with 0.1% Tris-buffered saline/Tween buffer and incubated with the appropriate HRP-conjugated secondary antibodies. The proteins were then detected using an ECL Plus kit (GE Healthcare) and visualized in an X-ray developer. To ensure equal protein loading, the same blot was stripped with stripping buffer [25 mM glycine and 1% SDS (pH 2.0)] and then incubated with an HRP-conjugated anti-mouse β -actin antibody. Protein band intensities were quantified using ImageJ software (NIH).

RNA Sequencing and Bioinformatics Analysis. RNA isolated from primary podocytes (P0) was purified using a RNeasy Plus Mini Kit (Qiagen). RNA quality was assessed using a Bioanalyzer kit (Agilent Technologies), and only samples with an RNA integrity number above 9 were used for cDNA production. The library was prepared from RNA (30 ng) using a SMARTer PCR cDNA synthesis kit (Clontech). Single-end 50-bp sequencing was performed using an Illumina HiSeq3000 system, and the sequencing performance was assessed with RSeQC version 2.3. Reads were aligned to the Ensembl release 76 assembly with STAR version 2.0.4 b. Gene counts were derived from the number of uniquely aligned unambiguous reads by Subread (featureCounts version 1.4.5). All gene counts were then imported into the R/Bioconductor package EdgeR, and trimmed mean of M (TMM) value normalization size factors were calculated to adjust for samples for differences in library size. The TMM size factors and the matrix of counts were then imported into the R/Bioconductor package Limma to test for differential gene expression between Tg-WT ($n = 4$) and Tg-C321R ($n = 3$) mice. GSEA was used to test pathway enrichment for differentially expressed genes (30), and the R/Bioconductor package pathview was utilized to generate pathway maps on known signaling and metabolism pathways curated by the KEGG.

Lentiviral Transduction of Primary Podocytes. The pLenti6.3 expression vectors encoding SERCaMP or GLuc-STOP have been described previously (35). The lentiviral vectors were packaged into virions in HEK 293T cells. In brief, 80% confluent HEK 293T cells were transfected with pLenti6.3-SERCaMP or pLenti6.3-GLuc-STOP and the 2 helper plasmids pMD2.G and psPAX2 (both from Addgene) in antibiotic-free DMEM with 10% FBS using Lipofectamine 2000 (Invitrogen), according to the manufacturer's protocol. After 18 h, the medium was changed to DMEM with 10% FBS and penicillin-streptomycin. At 24–48 h thereafter, the virus-containing cell culture supernatant was harvested, centrifuged at 1,000 rpm for 3 min, filtered through a 0.45- μ m filter (Millipore), and frozen at -80 °C. Primary podocytes from the re-

spective mice at P27 were transduced with the lentiviruses, which were titered using a Lenti-X p24 Rapid Titer Kit (Clontech), and used at a multiplicity of infection of 5.

Luciferase Assay. Primary podocytes from Tg-WT, Tg-C321R, and *Lamb2*^{+/-} mice at P27 were cultured on collagen I-coated 12-well plates at 1.2×10^4 cells per well and transduced with lentiviruses expressing SERCaMP or GLuc-STOP for 8 h. At 48 h thereafter, the Gluc activity in the media from the transduced podocytes was assayed by a BioLux *Gaussia* Luciferase Assay Kit (New England Biolabs) according to the manufacturer's instructions and quantified with a Femtomaster FB12 Luminometer (Zylux). The actual values of raw light units were normalized with respect to total cell protein for each group.

Urinary calpain activity was measured by Calpain-Glo Protease Assay (Promega). In brief, urine samples were incubated with calpain substrate (succinyl-LLVY-aminoluciferin). Following cleavage of substrate by calpain, the substrate for luciferase (aminoluciferin) was released, allowing the luciferase reaction to occur and luminescence to be detected by a Femtomaster FB12 Luminometer. The actual values of raw light units were normalized by urine Cr for each group.

Measurement of Cytosolic Calcium Levels. The cytosolic Ca²⁺ levels were measured by Fluo-4 AM (Invitrogen). Primary podocytes of the indicated genotypes were plated on 6-well plates at 1×10^5 cells per well and stained with 2.5 μ M Fluo-4 AM and 1 mM probenecid in the dark at 37 °C for 30 min. Then, the cells were washed with phosphate-buffered saline (PBS) and kept in the dark for another 30 min to allow cleavage of intracellular AM esters. Fluorescence was measured by a Calibur 3 flow cytometer (BD Biosciences) at the fluorescence-activated cell sorting core facility of the Washington University School of Medicine. The results were analyzed by the CellQuest program. For measuring intracellular Ca²⁺ levels in primary podocytes treated with or without K201 or MANF, cells were plated on 96-well plates at 0.8×10^4 cells per well and stained with Fluo-4 AM along with probenecid to enable high-throughput readout. Fluorescence was measured at an excitation wavelength of 485 nm and emission wavelength of 528 nm by a Synergy H1 fluorescent plate reader (BioTek).

Apoptosis Analysis in Primary Podocytes. Apoptotic cell death was measured by a fluorescein isothiocyanate (FITC)-Annexin V/PI apoptosis detection kit (BD Biosciences) according to the manufacturer's protocol. Primary podocytes from the indicated genotypes were plated on 6-cm dishes at 1.5×10^5 cells per dish in the absence or presence of K201 or MANF for 24 h. The untreated and treated podocytes were harvested, washed with cold PBS twice, resuspended in binding buffer, and stained with FITC-Annexin V and PI in the dark at room temperature for 15 min. After incubation, binding buffer was added and the podocytes were analyzed by a Calibur 3 flow cytometer (BD Biosciences). Unstained cells and cells stained with FITC-Annexin V or PI alone were used as controls to set up compensation and quadrants in flow cytometry. The results were analyzed by the CellQuest program.

Urinalysis. Mouse urine samples were collected by manual restraint or using a metabolic cage. The mouse urine samples were centrifuged at 1,800 \times g for 10 min to remove debris before being frozen at -70 °C. Urinary Cr concentration was quantified by a QuantiChrom Cr assay kit (DICT-500; BioAssay Systems), and albuminuria was measured by a QuantiChrom bacillus Calmette-Guérin albumin assay kit (DIAG-250; BioAssay Systems).

BUN Measurement. BUN was measured by using a QuantiChrom urea assay kit (DIUR-500; BioAssay Systems).

Statistics. Statistical analyses were performed using GraphPad Prism 5 software. Data were expressed as the mean \pm SD of 3 or more independent experiments. A 2-tailed Student's *t* test was used to compare two groups. One-way ANOVA with a post hoc Tukey test was used to compare multiple groups. $P < 0.05$ was considered statistically significant. The statistical analysis for RNA sequencing was as described above.

ACKNOWLEDGMENTS. We thank the Mouse Genetics Core, Washington University Center for Kidney Disease Research (NIH Grant P30DK079333) and Washington University Diabetes Research Center (NIH Grant P30 DK020579) for generation of Tg mice, as well as the Musculoskeletal Research Center Morphology Core (supported by NIH Grant P30AR074992) for histology. Mice were housed in a facility supported by NIH Grant C06RR015502. The pLenti6.3 SERCaMP and pLenti6.3 Gluc-STOP vectors were generous gifts from Dr. Brandon K. Harvey (NIH/NCATS). M.J.H. and S.M.Y. were supported

by the NCATS intramural research program. M.L. was supported by Juvenile Diabetes Research Foundation Grants 17-2013-410 and 2-SRA-2018-496-A-B, grants from the Finnish Diabetes Research Foundation, and Grant 117044 from the Academy of Finland. F.U. was supported by NIH Grants R01 DK112921 and UH2 TR002065. Y.M.C. was supported by NIH Grants R01 DK105056A1, R03DK106451, and K08DK089015; the Office of the Assistant Secretary of Defense for Health Affairs through the Peer Reviewed Medical Research Program under Award W81XWH18PRMRPIIRA; a Halpin Foundation-American Society of Nephrology Research Grant; a Faculty Scholar Award (MD-

FR-2013-336) from the Children's Discovery Institute of Washington University and St. Louis Children's Hospital; a Clinical Scientist Development Award (2015100) from the Doris Duke Charitable Foundation; a Career Development Award from the Nephrotic Syndrome Study Network; an Early Career Development Award from the Central Society for Clinical and Translational Research; and a Renal Translational Innovation Grant from the Washington University Division of Nephrology. Y.M.C. is a member of the Washington University Institute of Clinical and Translational Sciences (UL1 TR000448).

- M. Cozzolino *et al.*, Blood pressure, proteinuria, and phosphate as risk factors for progressive kidney disease: A hypothesis. *Am. J. Kidney Dis.* **62**, 984–992 (2013).
- S. Hoffmann, D. Podlich, B. Hänel, W. Kriz, N. Gretz, Angiotensin II type 1 receptor overexpression in podocytes induces glomerulosclerosis in transgenic rats. *J. Am. Soc. Nephrol.* **15**, 1475–1487 (2004).
- J. Reiser *et al.*, TRPC6 is a glomerular slit diaphragm-associated channel required for normal renal function. *Nat. Genet.* **37**, 739–744 (2005).
- R. Sonneveld *et al.*, Sildenafil prevents podocyte injury via PPAR- γ -Mediated TRPC6 inhibition. *J. Am. Soc. Nephrol.* **28**, 1491–1505 (2017).
- M. P. Winn *et al.*, A mutation in the TRPC6 cation channel causes familial focal segmental glomerulosclerosis. *Science* **308**, 1801–1804 (2005).
- L. Ellgaard, A. Helenius, Quality control in the endoplasmic reticulum. *Nat. Rev. Mol. Cell Biol.* **4**, 181–191 (2003).
- S. Munro, H. R. Pelham, An Hsp70-like protein in the ER: Identity with the 78 kd glucose-regulated protein and immunoglobulin heavy chain binding protein. *Cell* **46**, 291–300 (1986).
- J. Ye *et al.*, ER stress induces cleavage of membrane-bound ATF6 by the same proteases that process SREBPs. *Mol. Cell* **6**, 1355–1364 (2000).
- H. P. Harding *et al.*, Regulated translation initiation controls stress-induced gene expression in mammalian cells. *Mol. Cell* **6**, 1099–1108 (2000).
- H. Yoshida, M. Oku, M. Suzuki, K. Mori, pXBP1(U) encoded in XBP1 pre-mRNA negatively regulates unfolded protein response activator pXBP1(S) in mammalian ER stress response. *J. Cell Biol.* **172**, 565–575 (2006).
- T. Drozdova, J. Papillon, A. V. Cybulsky, Nephin missense mutations: Induction of endoplasmic reticulum stress and cell surface rescue by reduction in chaperone interactions. *Physiol. Rep.* **1**, e00806 (2013).
- Q. Fan *et al.*, R168H and V165X mutant podocin might induce different degrees of podocyte injury via different molecular mechanisms. *Genes Cells* **14**, 1079–1090 (2009).
- L. Liu *et al.*, Defective nephrin trafficking caused by missense mutations in the NPHS1 gene: Insight into the mechanisms of congenital nephrotic syndrome. *Hum. Mol. Genet.* **10**, 2637–2644 (2001).
- Y. M. Chen *et al.*, Laminin β 2 gene missense mutation produces endoplasmic reticulum stress in podocytes. *J. Am. Soc. Nephrol.* **24**, 1223–1233 (2013).
- A. V. Cybulsky *et al.*, Glomerular epithelial cell injury associated with mutant alpha-actinin-4. *Am. J. Physiol. Renal Physiol.* **297**, F987–F995 (2009).
- M. Pieri *et al.*, Evidence for activation of the unfolded protein response in collagen IV nephropathies. *J. Am. Soc. Nephrol.* **25**, 260–275 (2014).
- C. Gast *et al.*, Collagen (COL4A) mutations are the most frequent mutations underlying adult focal segmental glomerulosclerosis. *Nephrol. Dial. Transplant.* **31**, 961–970 (2016).
- L. Papazachariou *et al.*, Frequency of COL4A3/COL4A4 mutations amongst families segregating glomerular microscopic hematuria and evidence for activation of the unfolded protein response. Focal and segmental glomerulosclerosis is a frequent development during ageing. *PLoS One* **9**, e115015 (2014).
- J. Heymann, C. A. Winkler, M. Hoek, K. Susztak, J. B. Kopp (2017) Therapeutics for APOL1 nephropathies: Putting out the fire in the podocyte. *Nephrol. Dial. Transplant.* **32** (suppl. 1), i65–i70.
- M. F. Bek *et al.*, Expression and function of C/EBP homology protein (GADD153) in podocytes. *Am. J. Pathol.* **168**, 20–32 (2006).
- D. Mekahli, G. Bultynck, J. B. Parys, H. De Smedt, L. Missiaen, Endoplasmic-reticulum calcium depletion and disease. *Cold Spring Harb. Perspect. Biol.* **3**, a004317 (2011).
- M. Fill, J. A. Copello, Ryanodine receptor calcium release channels. *Physiol. Rev.* **82**, 893–922 (2002).
- H. Takeshima *et al.*, Generation and characterization of mutant mice lacking ryanodine receptor type 3. *J. Biol. Chem.* **271**, 19649–19652 (1996).
- Y. Kim *et al.*, Mesencephalic astrocyte-derived neurotrophic factor as a urine biomarker for endoplasmic reticulum stress-related kidney diseases. *J. Am. Soc. Nephrol.* **27**, 2974–2982 (2016).
- J. H. Miner, G. Go, J. Cunningham, B. L. Patton, G. Jarad, Transgenic isolation of skeletal muscle and kidney defects in laminin beta2 mutant mice: Implications for pierson syndrome. *Development* **133**, 967–975 (2006).
- I. Vermes, C. Haanen, H. Steffens-Nakken, C. Reutelingsperger, A novel assay for apoptosis. Flow cytometric detection of phosphatidylserine expression on early apoptotic cells using fluorescein labelled Annexin V. *J. Immunol. Methods* **184**, 39–51 (1995).
- X. Tian *et al.*, Podocyte-associated talin1 is critical for glomerular filtration barrier maintenance. *J. Clin. Invest.* **124**, 1098–1113 (2014).
- S. Lehtonen *et al.*, Cell junction-associated proteins IQGAP1, MAGI-2, CASK, spectrins, and alpha-actinin are components of the nephrin multiprotein complex. *Proc. Natl. Acad. Sci. U.S.A.* **102**, 9814–9819 (2005).
- J. Peltier *et al.*, Calpain activation and secretion promote glomerular injury in experimental glomerulonephritis: Evidence from calpastatin-transgenic mice. *J. Am. Soc. Nephrol.* **17**, 3415–3423 (2006).
- A. Subramanian *et al.*, Gene set enrichment analysis: A knowledge-based approach for interpreting genome-wide expression profiles. *Proc. Natl. Acad. Sci. U.S.A.* **102**, 15545–15550 (2005).
- R. E. Tunwell, F. A. Lai, Ryanodine receptor expression in the kidney and a non-excitable kidney epithelial cell. *J. Biol. Chem.* **271**, 29583–29588 (1996).
- X. H. Wehrens *et al.*, Ryanodine receptor/calcium release channel PKA phosphorylation: A critical mediator of heart failure progression. *Proc. Natl. Acad. Sci. U.S.A.* **103**, 5111–5118 (2006).
- J. Shan *et al.*, Role of chronic ryanodine receptor phosphorylation in heart failure and β -adrenergic receptor blockade in mice. *J. Clin. Invest.* **120**, 4375–4387 (2010).
- J. Shan *et al.*, Phosphorylation of the ryanodine receptor mediates the cardiac fight or flight response in mice. *J. Clin. Invest.* **120**, 4388–4398 (2010).
- M. J. Henderson, E. S. Wires, K. A. Trychta, C. T. Richie, B. K. Harvey, SERCaMP: A carboxy-terminal protein modification that enables monitoring of ER calcium homeostasis. *Mol. Biol. Cell* **25**, 2828–2839 (2014).
- C. C. Glembotski *et al.*, Mesencephalic astrocyte-derived neurotrophic factor protects the heart from ischemic damage and is selectively secreted upon sarco/endoplasmic reticulum calcium depletion. *J. Biol. Chem.* **287**, 25893–25904 (2012).
- M. J. Henderson, C. T. Richie, M. Airavaara, Y. Wang, B. K. Harvey, Mesencephalic astrocyte-derived neurotrophic factor (MANF) secretion and cell surface binding are modulated by KDEL receptors. *J. Biol. Chem.* **288**, 4209–4225 (2013).
- A. Apostolou, Y. Shen, Y. Liang, J. Luo, S. Fang, Armet, a UPR-upregulated protein, inhibits cell proliferation and ER stress-induced cell death. *Exp. Cell Res.* **314**, 2454–2467 (2008).
- N. Mizobuchi *et al.*, ARMET is a soluble ER protein induced by the unfolded protein response via ERSE-II element. *Cell Struct. Funct.* **32**, 41–50 (2007).
- K. Oh-Hashi, K. Tanaka, H. Koga, Y. Hirata, K. Kiuchi, Intracellular trafficking and secretion of mouse mesencephalic astrocyte-derived neurotrophic factor. *Mol. Cell. Biochem.* **363**, 35–41 (2012).
- A. Kushnir, A. R. Marks, The ryanodine receptor in cardiac physiology and disease. *Adv. Pharmacol.* **59**, 1–30 (2010).
- S. O. Marx *et al.*, Phosphorylation-dependent regulation of ryanodine receptors: A novel role for leucine/isoleucine zippers. *J. Cell Biol.* **153**, 699–708 (2001).
- U. D. Dincer, Cardiac ryanodine receptor in metabolic syndrome: Is JTV519 (K201) future therapy? *Diabetes Metab. Syndr. Obes.* **5**, 89–99 (2012).
- X. Liu *et al.*, Role of leaky neuronal ryanodine receptors in stress-induced cognitive dysfunction. *Cell* **150**, 1055–1067 (2012).
- X. H. Wehrens *et al.*, Protection from cardiac arrhythmia through ryanodine receptor-stabilizing protein calstabin2. *Science* **304**, 292–296 (2004).
- M. Lindahl *et al.*, MANF is indispensable for the proliferation and survival of pancreatic β cells. *Cell Rep.* **7**, 366–375 (2014).
- P. Petrova *et al.*, MANF: A new mesencephalic, astrocyte-derived neurotrophic factor with selectivity for dopaminergic neurons. *J. Mol. Neurosci.* **20**, 173–188 (2003).
- M. H. Voutilainen *et al.*, Mesencephalic astrocyte-derived neurotrophic factor is neurorestorative in rat model of Parkinson's disease. *J. Neurosci.* **29**, 9651–9659 (2009).
- M. Airavaara *et al.*, Mesencephalic astrocyte-derived neurotrophic factor reduces ischemic brain injury and promotes behavioral recovery in rats. *J. Comp. Neurol.* **515**, 116–124 (2009).
- P. Lindholm *et al.*, MANF is widely expressed in mammalian tissues and differentially regulated after ischemic and epileptic insults in rodent brain. *Mol. Cell. Neurosci.* **39**, 356–371 (2008).
- J. Neves *et al.*, Immune modulation by MANF promotes tissue repair and regenerative success in the retina. *Science* **353**, aaf3646 (2016).
- W. Yang *et al.*, Mesencephalic astrocyte-derived neurotrophic factor prevents neuron loss via inhibiting ischemia-induced apoptosis. *J. Neurol. Sci.* **344**, 129–138 (2014).
- National Research Council, *Guide for the Care and Use of Laboratory Animals* (National Academies Press, Washington, DC, ed. 8, 2011).